Separation and Purification Technology 382 (2026) 135814

Contents lists available at ScienceDirect

Separation and Purification Technology

journal homepage: www.elsevier.com/locate/seppur

Enhancement of the gas separation performance of mixed matrix membranes (MMMs) with functionalized triptycene hypercrosslinked polymers of intrinsic microporosity (HCP-PIMs)

Carmen Rizzuto [a], Haoli Zhou [b,c], Ariana R. Antonangelo [b], C. Grazia Bezzu [b], Johannes Carolus Jansen [a], Mariolino Carta [b,*], Alessio Fuoco [a,*]

[a] Institute on Membrane Technology, National Research Council of Italy (CNR-ITM), via P. Bucci 17/C, Rende, (CS), 87036, Italy
[b] Department of Chemistry, Faculty of Science and Engineering, Swansea University, Grove Building, Singleton Park, Swansea, SA2 8PP, UK
[c] State Key Laboratory of Materials-Oriented Chemical Engineering, College of Chemical Engineering, Nanjing Tech University, 5 Xinmofan Road, Nanjing 210009, PR China

ARTICLE INFO

Editor: Gaohong He

Keywords:
Gas separation
Transport properties
PIMs
Mixed matrix membranes
Hypercrosslinked polymers
Temperature dependence

ABSTRACT

In this work, we report a series of Matrimid®9725 based mixed matrix membranes (MMMs) containing 10 wt% and 20 wt% of highly microporous hypercrosslinked triptycene PIMs (HCP-PIMs) fillers. The latter were used either in their pristine hydrocarbon form, or functionalized with nitro, amino, or sulfonic groups. Single gas time-lag measurements show that the combination of the lowly permeable polymeric matrix and the highly porous fillers leads to an enhancement of gas selectivity (up to 29 % for CO_2/CH_4) and, depending on the filler, to an up to twofold increased permeability for CO_2. The selectivity increase seems influenced by the nature of the functional groups, while the permeability by the filler's high surface areas. Specifically, an enhancement of the permeability is observed across all MMMs, with the best results achieved with the hydrocarbon and the nitro functionalized HPC fillers (PIM-Trip-H and PIM-Trip-NO_2), which show an up to twofold increment of the permeability compared to the pure Matrimid, accompanied by a further improvement of the selectivity for gas pairs such as CO_2/CH_4 and O_2/N_2. Thermal studies show that permeability increases upon heating for all MMMs, while the selectivity decreases for gas pairs involving condensable gases such as CO_2. For instance, from 25 °C to 45 °C the permeability of CH_4 increases up to about 300 % and that of CO_2 only between 25 % and 50 %. Finally, the entropic and energetic contributions to diffusion selectivity are analyzed, providing insight into the varying influences of diffusivity and selectivity for different gases.

1. Introduction

Global warming is a persistent concern in modern society due to the significant threats it poses to the planet and all living species. Both academia and industry are tackling the crucial issue of separating and sequestering greenhouse gases that are evidently contributing to it, such as CO_2 and CH_4, with relative success [1–3]. In this context, membrane technology offers several advantages over other gas separation techniques (e.g., cryogenic distillation, absorption, pressure swing adsorption) [4–7], due to their higher energy efficiency, typically owed to the lower pressures and temperatures they operate, lower running costs and maintenance, because of the high gas flux of gas that can be treated at once [8,9], and their relatively high gas selectivity. This is crucial to prevent repeating the same separations several times before reaching the desired gas purity [10]. Because of these advantages, the membranes field is constantly expanding, and lately is especially focusing on the efficient separation and purification of gas mixtures that may come from natural sources [11,12], industrial production [13,14] and waste resources [15,16].

The performance of a gas separation membrane is evaluated by measuring the permeability of a gas a ($\boldsymbol{P_a}$, typically reported in Barrer, where 1 Barrer = 1 cm^3_{STP} cm cm^{-2} s^{-1} $cmHg^{-1}$), against its selectivity over a less permeable one b ($\boldsymbol{\alpha_{a,b}} = P_a/P_b$). A well-known trade-off exists between these two parameters, which states that if for a specific gas permeability increases its selectivity over another one decreases, and vice versa. A practical assessment of this trade-off was for the first time

* Corresponding authors.
E-mail addresses: mariolino.carta@swansea.ac.uk (M. Carta), alessio.fuoco@cnr.it (A. Fuoco).

https://doi.org/10.1016/j.seppur.2025.135814
Received 25 June 2025; Received in revised form 17 October 2025; Accepted 22 October 2025
Available online 25 October 2025

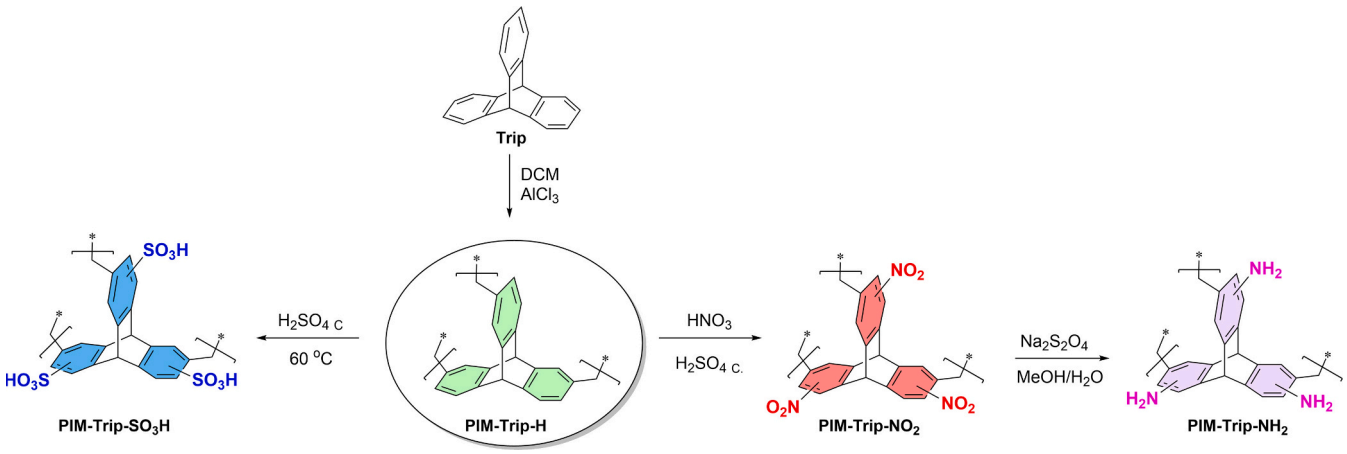

Fig. 1. Synthesis and functionalization of hypercrosslinked triptycene polymers.

proposed by Robeson in 1991, when he organized the best performing membranes for gas separation according to their permselectivity data and arranged them in double logarithmic plots [17]. He then selected commercially important gas pairs and for each plot he drew upper bounds, stating that materials that surpassed these empirical lines possess state-of-the-art performance. He then updated his own work in 2008 [18], when he introduced more polymers that systematically exceeded the previous limits. Since then, newer potential upper bounds were proposed by other researchers, such as Pinnau and co-workers who in 2015 set new limits for O_2/N_2, H_2/N_2 and H_2/CH_4 [19], and McKeown et al. who in 2019 established new boundaries for CO_2 based gas pairs (CO_2/CH_4 and CO_2/N_2) [20].

Commercial gas separation materials, including Matrimid®, Pebax®, and polysulfones, are typically preferred by the industry due to a combination of their cost vs performance [21–24]. However, they demonstrate low to moderate permeability and selectivity, which push researchers to search for more efficient systems. A recent solution designed to improve the poor performance of these commercial polymers, which are notoriously challenging to enhance and adjust for specific applications [25,26], involves the creation of more permeable mixed matrix membranes (MMMs). They are composite materials where a soluble polymer is blended with porous additives, which typically aims to enhance the overall permselectivity without increasing too much their costs, for instance by avoiding large amounts of the additive (10–20 wt%). A multitude of innovative and high-performing MMMs are regularly reported [27–29], frequently starting from commercially available polymers such as Matrimid®, which is probably the most commonly used polyimide (PI) for gas separation. This pristine polymer is a low-permeability/high-selectivity PI with $P_{CO2} \sim 10.8$ Barrer and $P_{CH4} \sim 0.35$ Barrer, with CO_2/CH_4 and CO_2/N_2 selectivities of 35 and 31, respectively [30]. Considering the poor permeability of neat Matrimid®, that hinders its use for the treatment of large-scale CO_2 capture processes such as from flue gas, it seems logical attempting to enhance its permeability using porous fillers, while maintaining decent selectivity [31,32]. This is crucial to ensure that large volumes of gases can be treated at once (high flux), enabling the separation process to maximize throughput without sacrificing selectivity (and thus purity).

Polymers of intrinsic microporosity (PIMs) form a class of porous material that has been successfully employed in various fields, such as catalysis [33], electrochemistry [34], and water purification [35]. However, they are best known for their exceptional performance as gas separation membrane materials [20,36,37]. Not only are they promising candidates for advancing the field when used as processable polymers, but they have also been shown to be highly effective as amorphous fillers for MMMs [38]. It would be particularly intriguing to combine the amorphous and insoluble PIMs, functionalized with basic or acidic substituents, with the similar amorphous structure of polyimides [39], to alter the polymer matrix's affinity for various gases following a like-dissolves-like principle. This approach could be used to fine-tune the permeability and selectivity for specific gas pairs, simultaneously improving both permeability and selectivity of Matrimid®.

In a recent study, we demonstrated that incorporating amino groups into hypercrosslinked PIMs enhances their affinity for CO_2, which is quite a common feature in carbon capture materials [40]. In the same work we found out that groups such as sulfonic and nitro also have a significant impact on the overall gas separation performance when utilized as insoluble powders. In this study, we employed all these functionalized PIMs to produce novel MMMs in combination with the commercial Matrimid® as the soluble matrix, anticipating that a similar trend would be found when used as fillers in membranes, designed for separating various commercially important gas pairs.

2. Materials and methods

Commercially available reagents, polymers and gases were used without further purification, and gases for permeation tests (H_2, He, O_2, N_2, CH_4 and CO_2) were supplied by Sapio at a minimum purity of 99.9995.

2.1. Synthesis and functionalization of the hypercrosslinked polymers of intrinsic microporosity (HCP-PIMs)

The synthesis and functionalization of the triptycene PIMs were carried out following our previously reported procedure, [40] where all the relevant characterization that assessed the correct presence of the added functional groups will be found (this includes ^{13}C SSNMR, FT-IR, thermal analysis and titration of the sulfonic groups, that showed values between 2 and 3 sulfonic groups per repeat units). More in detail, after synthesis and post-polymerization functionalization, all the insoluble polymers were thoroughly washed under reflux with a series of solvents, sequentially starting from ethanol, chloroform, THF, acetone, and methanol. All polymers were finally dried in a vacuum oven at 100 °C for 20 h. The synthesis started from the formation of the initial hydrocarbon-based polymer **PIM-Trip-H**, made via a Friedel-Craft polymerization of the commercial triptycene. This was subsequently nitrated with concentrated nitric acid to obtain **PIM-Trip-NO$_2$**. The amino polymer **PIM-Trip-NH$_2$** was synthesized via the reduction of the nitro material using sodium dithionite in methanol and water. Finally, the direct sulfonation of **PIM-Trip-H** with concentrated sulfuric acid at 60 °C afforded the last polymer, **PIM-Trip-SO$_3$H** (Fig. 1).

2.2. Membrane preparation

Prior to use, Matrimid®9725 and the HCP-PIMs were treated for at

least one night at 80 °C in a vacuum oven before the solution preparation. The pure Matrimid®9725 membrane and the MMMs containing 10 wt% or 20 wt% of the HCP-PIMs in Matrimid® were prepared casting the films from chloroform, all starting from a 3 wt/vol% solution. The neat 3 wt% Matrimid® solutions were left to stir overnight, filtered and cast by slow evaporation. For the MMMs, a controlled amount of the HCP-PIMs was added to the solution to produce the 10 wt% or 20 wt% HCP-PIM loaded suspensions. The Matrimid®9725/HCP-PIMs slurry was sonicated for 2 h using a sonication bath and then left to stir overnight. The day after they were sonicated again for 9 h before being cast into an 8 cm Teflon petri dish, from where the solvent was slowly allowed to evaporate at a temperature of 35 °C and ambient pressure for 3–5 days. The mixed matrix membranes are noted as: Matrimid®9725/Trip-A_B, where A is the name of the functional group on the PIM and B is the wt% of filler. For Instance, a membrane having 20 wt% of the PIM-Trip-H is reported as: Matrimid®9725/Trip -H_20.

2.3. Gas transport properties

Single gas permeation measurements were performed on circular membranes with a minimum exposed area of 2.14 cm^2 in the temperature range from 25 °C to 45 °C and at a feed pressure of 1 bar by a fixed volume/pressure increase instrument designed by HZG and constructed by EESR (Geesthacht, Germany). To obtain the complete desorption of all previously adsorbed gases and humidity, the measurement protocol involved that prior to each measurement the membrane sample was evacuated in the testing cell by a turbo-molecular pump for at least 4 h, and then, between two consecutive measurements, the membranes were evacuated for a time equal to at least 10 times the time lag of the previous gas. The time lag method was used for the determination of the permeability (P), diffusion (D), and solubility coefficients (S), following the increase of the permeate pressure p_t as a function of time t, immediately after the membrane was exposed to the gas as for (1).

$$p_t = p_0 + \left(\frac{dp}{dt}\right)_0 \times t + \frac{RT}{V_p \times V_m} \times A \times l \times p_f \times S \times \left(\frac{D \times t}{l^2} - \frac{1}{6} - \frac{2}{\pi^2}\sum_{n=1}^{\infty}\frac{(-1)^n}{n^2}\exp\left(-\frac{D \times n^2 \times \pi^2 \times t}{l^2}\right)\right) \quad (1)$$

where p_0 and $(dp/dt)_0$ are the starting pressure and baseline slope, respectively, and should be negligible. R is the universal gas constant, T the absolute temperature, V_p the permeate volume, V_m the molar volume of the gas, A is the membrane area l its thickness and p_f the feed pressure. The permeability coefficient (P) was calculated from permeate pressure increase rate dp/dt in the pseudo steady-state, where Eq. 1 reduces to (2):

$$P = \frac{V_P \times V_m \times l}{RT \times A \times p_f} \times \frac{dp}{dt} \quad (2)$$

The diffusion coefficient (D) is inversely proportional to time lag (Θ) and was calculated from (3):

$$\Theta = \frac{l^2}{6D} \quad (3)$$

According to the solution-diffusion model, the solubility coefficient (S) was calculated from (4):

$$S = P/D \quad (4)$$

3. Results and discussion

3.1. Synthesis and characterization of the polymers

The hypercrosslinked polymers reported in this paper are all based on the triptycene core, which has been previously employed in several works to create high-performing PIMs, both in soluble and networked (insoluble) forms. This core structure is particularly interesting as its trigonal "propeller-like" shape prevents the polymer chains from efficiently packing in the solid state, resulting in a high internal free volume (IFV) [41–43]. A further advantage of this core is the easy functionalization of its backbone, as the aromatic moieties are prone to promote electrophilic substitution, which allows for the introduction of substituents of different natures able to tune the selectivity of the polymeric structure for several gases [44]. All the polymers were obtained as highly porous networks, which facilitated their purification through simple washing of the obtained powder with different solvents, followed by vacuum filtration. The textural properties were evaluated through isothermal nitrogen adsorption at 77 K, and the surface areas calculated using BET theory finding the trend **PIM-Trip-H** (1880 m^2g^{-1}) > **PIM-Trip-SO$_3$H** (1145 m^2g^{-1}) > **PIM-Trip-NO$_2$** (975 m^2g^{-1}) > **PIM-Trip-**

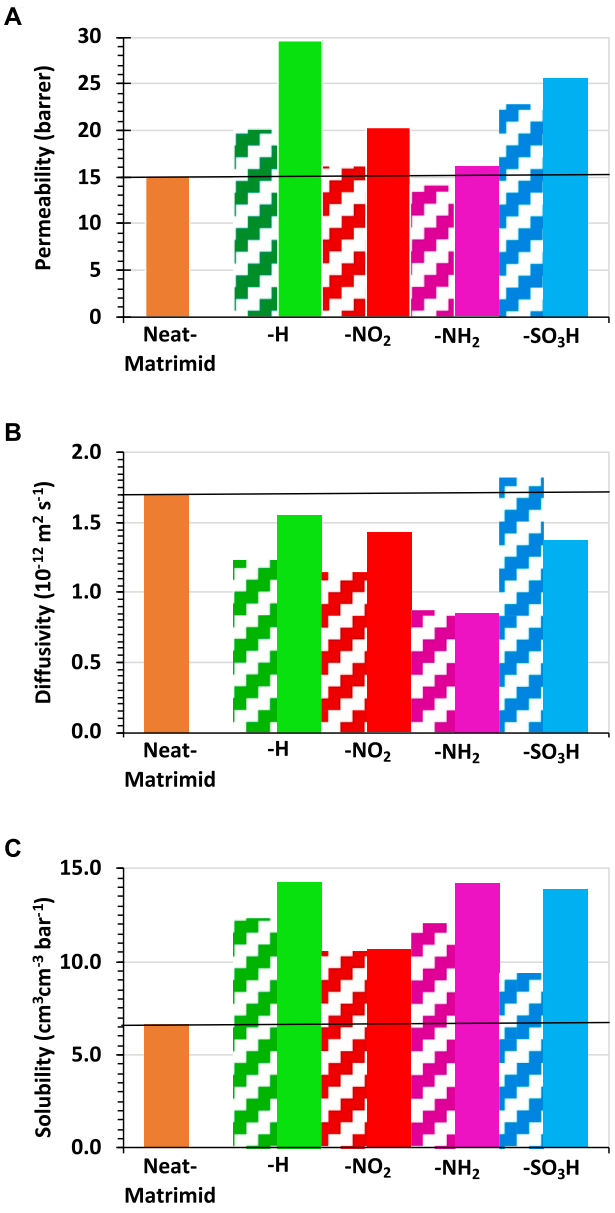

Fig. 2. Comparison of (a) permeability, (b) effective diffusivity and (c) effective solubility coefficients for CO_2 at 25 °C in the neat-Matrimid®9725 (orange series), Matrimid®9725/Trip-H MMMs (green series), Matrimid®9725/Trip-NO_2 MMMs (red series), Matrimid®9725/Trip-SO_3H MMMs (blue series), Matrimid®9725/Trip-NH_2 MMMs (magenta series), as function of the different concentrations of the fillers (10 wt% pale colour and 20 wt% bright colour).

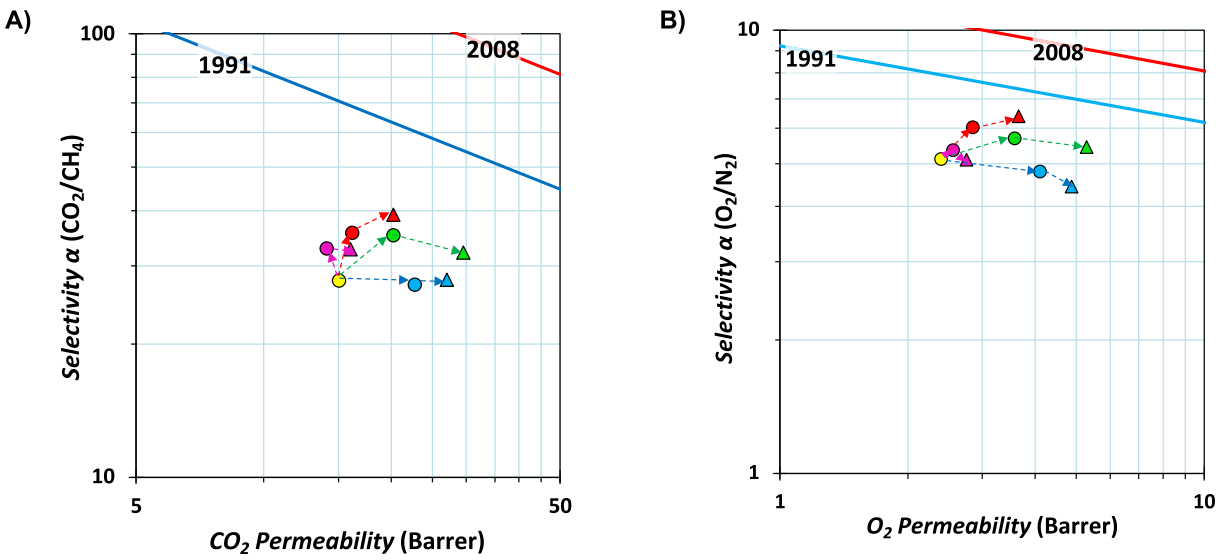

Fig. 3. Robeson diagrams for the (**a**) CO_2/CH_4 and (**b**) O_2/N_2, gas pairs with the upper bounds represented by blue lines for 1991, and red lines for 2008. The gas permeabilities are reported for neat Matrimid®9725 in yellow circles •, for Matrimid®9725/Trip-H in green (circle ● 10 wt% and triangle ▲ 20 wt%), for Matrimid®9725/Trip-NO_2 in red (circle ● 10 wt% and triangle ▲ 20 wt%), for Matrimid®9725/Trip-NH_2 in pink (circle ● 10 wt% and triangle ▲ 20 wt%), for Matrimid®9725/Trip-SO_3H in blue (circle ● 10 wt% and triangle ▲ 20 wt%).

NH_2 (610 m^2g^{-1}). CO_2, CH_4 and N_2 adsorption measurements at different temperatures (273 and 298 K) were also performed, proving that these hypercrosslinked polymers are quite selective for CO_2 over N_2 and CH_4, as reported in our previous paper [40], with the best CO_2 uptakes shown by the sulfonated polymer, and the best IAST selectivities for CO_2 over N_2 or CH_4 displayed by the nitro and aminated ones. It is worth noting that, despite the hydrocarbon polymer displayed the highest BET surface area, the functionalized polymers exhibited both higher CO_2 adsorption and better selectivity, thus demonstrating the significant influence that substituents have on these materials. Post-polymerization modifications showed the expected reduction of porosity, but the extent varied by functional group. Polymers with nitro or sulfonic groups retained substantial porosity, while aminated polymers (PIM-NH_2) showed greater loss due to likely hydrogen bonding between chains. This suggests that amines more significantly reduce internal free volume by promoting polymer chain interactions beyond simple pore-filling and enhanced hydrogen bonding [45,46].

3.2. Membrane preparation and characterization

The successful formation of defect free self-standing mixed matrix membranes required a long sonication time (> 10 h in a sonication bath) to allow for the best possible dispersion of the HCP-PIM particles in the polymer solution. Previous attempts with lower sonication time, (i.e., 3 and 6 h), always led to the formation of non-uniform membranes with visible aggregation of HCP-PIMs. Long sonication times, instead, permitted the preparation of homogeneous dispersions by breaking large clusters before casting. To ensure that extended sonication times did not affect the chemical structures of either the polymer matrix or the fillers, we conducted stability tests, by analyzing the Matrimid by ^1H NMR and the Trip-SO_3H filler by isothermal CO_2 adsorption at 273 K before and after sonication. We specifically selected the latter test for the filler, as we deemed the sulfonic acid groups to be the most likely to be affected by prolonged sonication. The results confirmed that both components remained chemically unchanged. Figure SI 1 reports SEM images of the produced membranes showing their homogeneity and good filler dispersion. Optical photographs confirm homogeneity also at macroscopic scale as well as their flexibility.

3.3. Single gas transport properties

In general, for the prepared MMMs we noticed that the addition of HCP-PIMs leads to an increase in the CO_2 permeability compared to neat Matrimid®, especially at higher filler concentration (Fig. 2a). The increase in permeability is generally attributed to a combination of changes in solubility and diffusivity. In our case, however, the diffusivity coefficient shows only a modest enhancement, observed exclusively for the MMM containing 10 wt% sulfonated filler (Fig. 2b), when compared to the neat Matrimid. However, more than the effective diffusion coefficient, the boost of the apparent CO_2 solubility coefficient (Fig. 2c) seems playing the main role in these systems in all the produced MMMs, as the addition of the HCP-PIMs shows a reduction of the effective diffusion coefficients (Figure SI 2), while the CO_2 solubility increases. This effect is likely due to the combination of two separate factors: i) the increased overall CO_2 affinity, due to noncovalent interactions, leads an "immobilizing effect" and ii) the presence of additional free volume acts as a "buffer" and slows down the diffusion. Similar effects have been observed in other MMMs [47] where the low diffusion coefficient may be attributed to so-called "immobilizing sorption" [48,49], and in Amine-PIM-1, where the immobilizing sorption is due to a reversible reaction of CO_2 with the amino groups of the PIM, forming the corresponding carbamic acid [50].

The fillers also have a strong impact on the general gas selectivity, and this can be attributed to the nature of the functional groups, as possible to assess from the Robeson plots (Fig. 3 and Figure SI 1). As already displayed in Fig. 2, the MMMs with Trip-H and Trip-SO_3H show the strongest increase in permeability, but the latter shows a higher CO_2/CH_4 and O_2/N_2 selectivity, while selectivity of the samples with Trip-H remains equal or decreases slightly. For the same gas pairs, the permeability of Trip-NO_2 also increases but somewhat less significantly, while its selectivity shows the strongest increase of the entire set. Thus, despite a relatively lower permeability enhancement, compared to other functionalized HCP-PIMs, the introduction of the nitro groups leads to a higher increase in selectivity, which might be due to the filler peculiar adsorption mechanism that fits in between physisorption and chemisorption [40], as also seen in nitrate MOFs [51]. Surprisingly, the aminated version of the HCP-PIM shows hardly any changes or even slightly reduced performance compared to the other fillers, although the presence of the nucleophilic site was expected to induce a higher affinity for

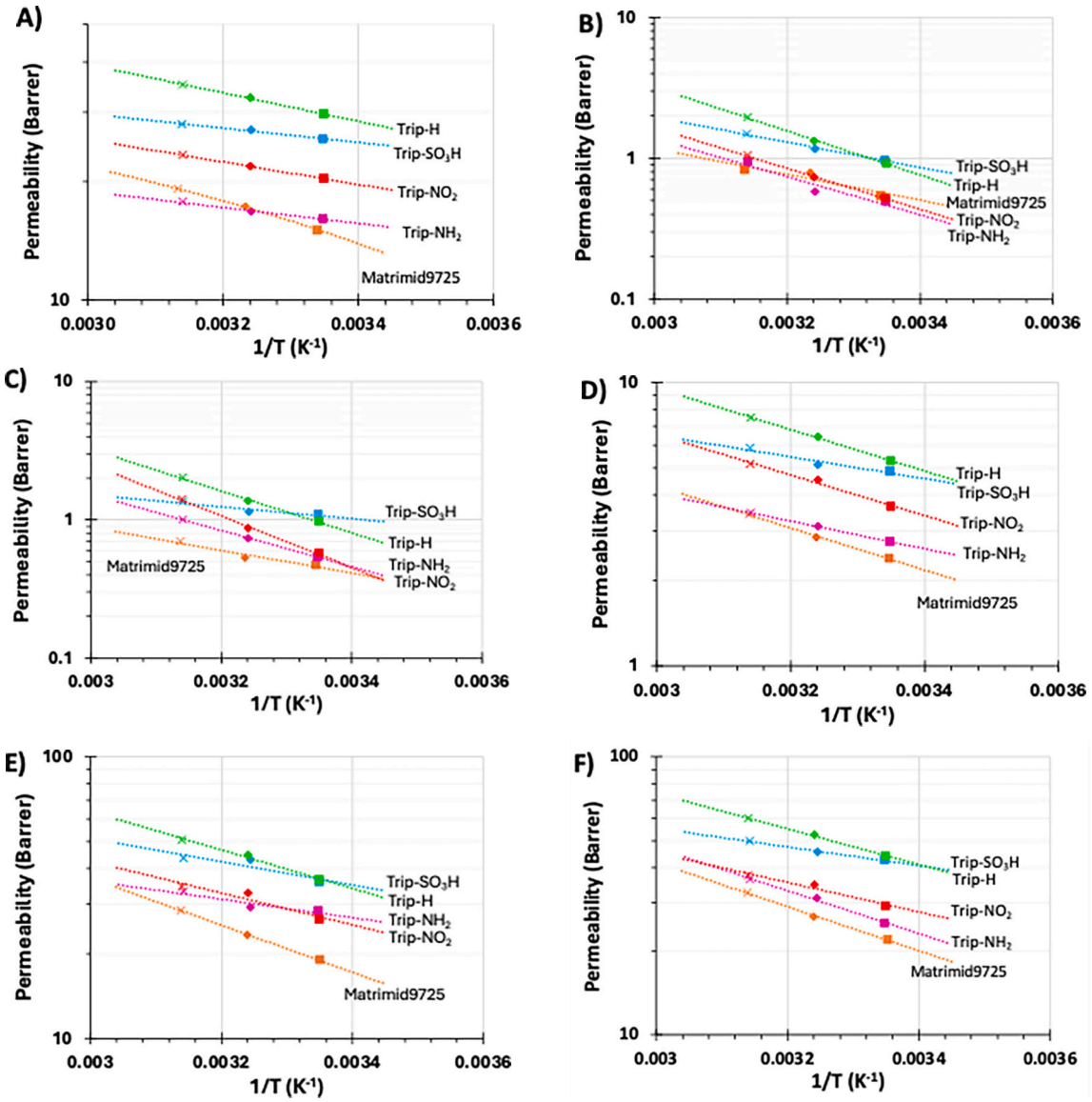

Fig. 4. Arrhenius plot of the permeability for CO_2 (A), CH_4 (B), N_2 (C), O_2 (D), He E), and H_2 (F), as a function of the inverse of the temperature for neat Matrimid®9725 (orange series), Matrimid®9725/Trip-H_20 (green series), Matrimid®9725/Trip-NH_2_20. (magenta series), Matrimid®9725/Trip-NO_2_20 (red series), and Matrimid®9725/Trip-SO_3H_20 (blue series) Numerical data associated to this figure are reported in the SI.

CO_2. The lower performance could be attributed to two key factors: i) the decrease of the filler's porosity, as the introduction of the -NH_2 reduces the fractional free volume (FFV) available for gas sorption and diffusion [40], and ii) the presence of the amino groups induces strong interactions with carbon dioxide, which in turn increase the solubility of CO_2 and simultaneously hinders its diffusion [50,52]. Indeed, the Trip-NH_2 filler exhibits a marked increase in CO_2 affinity (Fig. 2c). While this enhancement is accompanied by only a modest decrease in effective diffusivity for the Trip-H, Trip-NO_2, and Trip-SO_3H (at 20 wt%), the incorporation of Trip-NH_2 leads to a more pronounced reduction in the diffusion coefficient, similar to the effect previously observed with Amine-PIM-1 [50]. However, with exception of Trip-SO_3H, which shows an enhancement of the effective diffusion coefficient at 20 wt%, all other fillers produce a general reduction of the effective diffusivity (Fig. 2b). The effect is strongest for CO_2, which may be due to its higher affinity for Trip-NH_2. The fact that also nonpolar, non-condensable gases (Figure SI 3, Figure SI 6) show similar behavior, suggests that the filler simply provides a higher fractional free volume, which takes longer to be saturated by the permeating gas. This is somewhat counter-intuitive, but it actually leads to the increase of the time lag, thus reducing the effective diffusion coefficient, even in cases where the permeability is hardly affected [47].

In general, the Matrimid®9725/Trip-NO_2 series moves the performance towards the upper-right side of the Robeson upper bound (Fig. 3 and Figure SI 1), which is ideal as it shows the best trade-off between increase in permeability and selectivity for many gas pairs, for both effective solubility (e.g., CO_2/CH_4, CO_2/N_2) or effective diffusivity (e.g., O_2/N_2, H_2/N_2) driven separations. As discussed above, this combination reaches the highest selectivity among all fillers, albeit at somewhat lower permeabilty, but this may be an advantage for those applications where the final purity of the separated gas is more important than the total flow rate. A further advantage of this filler compared to others lies in its synthesis, as it requires one less synthetic step than PIM-Trip-NH_2 (the reduction), making the PIM-Trip-NO_2 a potentially better candidate for scale-up. The trends for CO_2/N_2 (Figure SI 1b) are similar to those of CO_2/CH_4 but the latter shows a slightly better selectivity at 20 wt% of the filler. Remarkably the H_2/N_2 gas pair (Figure SI 1a) exhibits a strong drop in selectivity upon increasing the filler content from 10 wt% to 20 wt%, mostly as a result of a stronger increase in N_2 permeability over H_2. This also suggests an increase in the fractional free volume, which

Table 1
Activation energy of Permeation (E_p, kcal mol^{-1}), of Diffusion (E_d, kcal mol^{-1}) and Heat of Sorption (H_s, kcal mol^{-1}) for the neat Matrimid and the mixed matrix membranes prepared with 20 wt% of the HCP-PIMs.

	Gas	Matrimid®	+ Trip-H_20	Trip-NO_2_20	+ Trip-NH_2_20	+ Trip-SO_3H_20
E_p	N_2	5.06	6.92	6.29	5.99	1.96
	O_2	3.20	3.34	3.27	2.23	1.75
	CO_2	1.98	1.65	1.31	0.92	0.83
	CH_4	4.83	7.14	6.63	6.19	4.07
	H_2	3.84	2.93	2.43	3.51	1.54
	He	4.00	3.12	2.58	1.50	1.90
E_d	N_2	7.46	8.41	8.48	7.46	7.22
	O_2	6.35	7.91	7.60	6.20	6.49
	CO_2	6.81	7.06	7.78	6.69	6.64
	CH_4	7.96	10.22	10.74	9.38	9.36
H_s	N_2	−2.41	−1.49	−2.19	−1.47	−5.26
	O_2	−3.16	−4.58	−4.33	−3.97	−4.74
	CO_2	−4.83	−5.41	−6.47	−5.77	−5.81
	CH_4	−3.14	−3.08	−4.11	−3.19	−5.28

enhances the permeability for all gases at the expense of the high original size-selectivity shown by the matrix polymer. Overall, the Trip-NO_2 filler seems to reach the best compromise due to enhanced affinity and diffusivity, while the Trip-H is the most effective in increasing permeability due to its high porosity, the highest of this family of fillers.

When compared to already reported high-performing Matrimid-based MMMs [27–29], the herein discussed MMMs show limited enhancement of the gas transport properties. However, due to their amorphous organic nature, they can be solution-processed to form the membrane/selective layer in thin film composite and do not require the additional thermal annealing process at high temperature that is a standard procedure when inorganic/crystalline filler are introduced in polymer matrix. This is a crucial aspect for the possible exploitation and scaling up of the membranes since the high temperature annealing process increases the energetic costs of the membrane production and limits the supports that can be used in the preparation of thin film composites.

3.4. Temperature dependence

Permeability measurements at temperatures ranging from 25 °C to 45 °C were conducted on MMMs prepared with 20 wt% filler loading. Measurements at higher temperatures were not performed since the MMMs were not stable over 50 °C probably due to defects at the interface between the polymer matrix and the filler, due to their different coefficient of thermal expansion. These measurements reveal that the permeability improves with the increase of the temperature for all gases (H_2, He, O_2, N_2, CH_4 and CO_2), with a somewhat steeper trend for the least permeable gases with larger molecular dimensions [53] such as N_2 and CH_4 (Fig. 4, and Table SI 1 and Table SI 2). This enhancement in permeability with the temperature was particularly evident for CH_4 and can be mostly attributed to a very steep increase of the effective diffusion coefficient (Figure SI 3c to Figure SI 7c). This, in turn, is due to the larger effective diameter of CH_4. Teplyakov and Meares [53] discussed that the diffusion coefficient decreases exponentially with the square of the effective gas diameter. This can be easily understood, considering that the cross-sectional area of a molecule determines its "friction" with the polymer matrix. On the other hand, CO_2 showed a much less significant change of the permeability vs. temperature (Fig. 4), despite having a similar effective diameter as N_2 [53].

The selectivity shows the opposite trend, with a reduction as a function of the temperature for the gas pairs CO_2/N_2, CO_2/CH_4, O_2/N_2 and CO_2/H_2 (Figure SI 4f to Figure SI -8f), with the strongest decrease in selectivity for the CO_2/CH_4 gas pair. All trends in permeability, diffusivity and solubility as a function of temperature follow typical Arrhenius behavior (Fig. 4 and Figure SI 4 to Figure SI 8) defined by the following equations (Eq. 5–7):

$$P = P_0 exp\left(\frac{-E_p}{RT}\right) \quad (5)$$

$$D = D_0 exp\left(\frac{-E_d}{RT}\right) \quad (6)$$

$$S = S_0 exp\left(\frac{-H_s}{RT}\right) \quad (7)$$

Where P_0, D_0 and S_0 are the pre-exponential factors, E_p is the activation energy of permeation, E_d the activation energy of diffusion, and H_s the heat of sorption. The parameters fitted with the Arrhenius equations are listed in Table 1. The steeper trend in P and D for CH_4 and the weaker trend for CO_2 originates from a higher activation energy for permeation for the larger gas molecules and a lower sorption enthalpy for CO_2.

The time lag of He and H_2 is too close to the instrumental limit to measure the diffusion coefficient (and indirectly) the solubility of these gases accurately. Therefore, the values of E_D and H_S could not be determined for these gases, but only E_p. Upon closer examination of the temperature-dependence data, we found that the variation in the diffusion coefficient closely follows the trend in permeability (Figure SI 3b to Figure SI 7b). The increase in effective diffusivity can be attributed to greater polymer chain mobility and improved gas molecule movement at higher temperatures. This leads to a reduced size-selectivity for most of the gas pairs (Figure SI 3c to Figure SI 7c). At the same time the solubility coefficients (Figure SI 3e to Figure SI 7e) and the solubility selectivity of most gas pairs (Figure SI 3f to Figure SI 7f) decrease with increasing temperature, and this can be directly correlated to the negative value of H_S in Eq. 7 (Table 1). As a result, the overall perm-selectivity declines with rising temperature for most gas pairs, due to reductions in both diffusion- and solubility-based selectivity (Figure SI 4 to Figure SI 8). The drop in solubility and selectivity is particularly pronounced when the highly condensable CO_2 is involved, as it has the most negative value of H_S among all gases. A fit of the data with the Arrhenius equations permits the extrapolation of the permeability and selectivity at higher or lower temperature with a reasonable level of confidence. Especially for CO_2/CH_4 separation, lower temperatures lead to a significantly higher selectivity, suggesting the potential use of these mixed matrix membranes in sub-ambient conditions [54].

The activation energy of permeation (E_p) of these membranes is within the same range as various other membrane forming polymers [55], particularly the high performing polypyrrolones [56]. In general, the addition of the fillers produces a reduction of E_p for CO_2 compared with neat Matrimid and, at the same time, it results in an increase of E_p for the other gas species, thus leading to a general improved selectivity. However, this trend is not observed for the MMMs based on Trip-SO_3H, since they show a lower E_p for all the gases, and this is correlated with a similar (or slightly lower) selectivity than the neat polymer. The addition of the fillers also produces an increment of the absolute values of the heat of sorption (H_s) for all MMMs, suggesting a higher membrane-gas affinity. In fact, H_s reflects on both this interaction and the temperature dependence of the solubility trend displayed in Fig. 2d.

The high activation energies of diffusion (E_d) for all gases suggests a high energy barrier of the gas diffusion that can be associated with improved diffusion selectivity, especially considering gases with particularly large values of E_d, such as CH_4. The addition of fillers increases E_d compared to the neat Matrimid. While the values relative to O_2 fall within the range of polypyrrolones (5–8 kcal mol^{-1}) [56], and those relative to CH_4 are even higher than in the highly size-selective PIM-BTrip (8.78 kcal mol^{-1}) [57]. This is an indication that diffusion plays a major role in the separation properties of such membranes. A deeper insight comes from the transition theory of diffusion, since the diffusion selectivity can be deconvoluted in two terms, one related to the energy needed to open motion-enabled zones of diffusion (the energetic

Table 2
Contribution of the energetic selectivity and the entropic selectivity to the diffusion selectivity for the neat Matrimid®9725, Matrimid®9725/Trip-H_20, Matrimid®9725/Trip-NO_2_20, Matrimid®9725/Trip-NH_2_20 and Matrimid®9725/Trip-SO_3H_20 membranes.

	Gas (A)	Matrimid®	+ Trip-H_20	+ Trip-NO_2_20	+ Trip-NH_2_20	+ Trip- SO_3H_20
Diffusion selectivity (A/N_2)	O_2	3.08	3.02	4.01	4.34	2.24
	CO_2	0.78	0.76	0.75	0.77	0.49
	CH_4	0.22	0.18	0.19	0.22	0.16
Energetic selectivity (A/N_2)	O_2	6.48	2.32	4.40	8.43	3.45
	CO_2	3.02	9.84	3.27	3.68	2.69
	CH_4	0.43	0.05	0.02	0.04	0.03
Entropic selectivity (A/N_2)	O_2	0.53	1.44	1.01	0.57	0.72
	CO_2	0.26	0.08	0.23	0.21	0.18
	CH_4	0.48	3.42	8.25	5.19	5.25

term), and another related to the thermodynamics of the process and the changes in the degrees of freedom of the gases during the diffusion.

According to the transition theory of diffusion, the diffusion selectivity between two gases a and b (D_a/D_b) can be defined as:

$$\frac{D_a}{D_b} = \frac{\lambda_a^2}{\lambda_b^2} \underbrace{exp\left(\frac{\Delta S_{d(a,b)}}{R}\right)}_{entropic\ selectivity} \underbrace{exp\left(-\frac{\Delta E_{d(a,b)}}{RT}\right)}_{energetic\ selectivity} \quad (8)$$

where λ_a and λ_b are the average diffusive jumps for gas a and b; $\Delta S_{d(a,b)}$ is the difference in the activation entropy of diffusion that defines the entropic selectivity; and $\Delta E_{d(a,b)}$ is the difference in the activation energies of diffusion, which influences the energetic selectivity. The values of λ_a and λ_b are generally unknown for a membrane, especially for mixed matrix membranes, but the ratio λ_a^2/λ_b^2 can be approximated as d_a^2/d_b^2, where d is the effective diameter of the penetrant gas. Analysis of the transport in terms of Eq. 8 provides fundamental understanding of the permselective properties of polymeric or mixed matrix membranes [58].

Although there are some outliers, the general trend indicates that the addition of HCP-PIMs enhances the diffusion selectivity for the O_2/N_2 gas pair (Table 2), while it does not virtually influence the CO_2/N_2. Indeed, the effective gas diameters of CO_2 and N_2, defined by Teplyakov and Meares [53] on the basis of a calibration with a range of noble gas molecules are remarkably similar and size-selectivity is usually very small for this gas pair. Moreover, the addition of the fillers decreases the energetic selectivity factor (Table 2), probably since preferential pathways for diffusion are provided by the highly porous fillers in the polymer/HCP-PIM mixed matrix membranes. At the same time, the entropic contribution on the O_2/N_2 diffusion selectivity can be mathematically considered as "medium" since it is close to 1. This means that both molecules experience similar changes in the degree of freedom when diffusing into the membrane.

4. Conclusions

In this work, we have shown the improvement of the performance of the low free volume glassy polyimide Matrimid®9725, via the preparation of mixed matrix membranes incorporating high free volume hypercrosslinked PIMs as fillers. Defect-free membranes can be obtained only with excellent dispersion of the fillers in the solution, which is facilitated by long sonication time of the dispersion of the two components before casting the film. The gas transport properties resulted heavily influenced by structural properties of the fillers and, while the permeability increases with increasing porosity, the selectivity seems more influenced by the different functional groups attached to the HCP-PIMs. Remarkably, the Trip-NO_2 filler proved to be very interesting in terms of performance, since it leads to an increase in both permeability and selectivity and also from the synthesis point of view, as it can be easily prepared by nitration of the hydrocarbon and requires one less step compared to the -NH_2 version. This is particularly significant, as the aminated version was expected to perform better due to the amino groups' enhanced affinity for mildly acidic gases like CO_2. Overall, Trip-NO_2 offers the best balance between improved solubility, due to higher affinity, and enhanced diffusivity resulting from its intrinsic porosity, while requiring fewer steps for its synthesis. Instead, Trip-H, which displays the highest porosity among these fillers, is most effective in increasing permeability.

Finally, by applying the Arrhenius equation, the permeability and selectivity data can be readily extrapolated with a reasonable level of confidence to both higher and/or lower temperature, suggesting stronger separation performance at sub-ambient conditions, and making these materials particularly promising for applications such as for carbon capture, biogas upgrading and flue gas purification. Overall, we believe that the HCP-PIMs discussed here, and especially the HCP-PIM-based MMMs, have potential applications in a variety of membrane-based separation processes.

CRediT authorship contribution statement

Carmen Rizzuto: Writing – review & editing, Writing – original draft, Investigation. **Haoli Zhou:** Writing – review & editing, Investigation. **Ariana R. Antonangelo:** Writing – review & editing, Investigation. **C. Grazia Bezzu:** Writing – review & editing. **Johannes Carolus Jansen:** Writing – review & editing, Resources. **Mariolino Carta:** Writing – review & editing, Writing – original draft, Supervision, Resources, Project administration, Investigation, Funding acquisition, Conceptualization. **Alessio Fuoco:** Writing – review & editing, Writing – original draft, Supervision, Resources, Project administration, Methodology, Investigation, Funding acquisition, Data curation, Conceptualization.

Declaration of competing interest

The authors declare the following financial interests/personal relationships which may be considered as potential competing interests: Fuoco and Jansen reports financial support was provided by European Commission. Bezzu and Carta reports financial support was provided by UK Research and Innovation. Carta and Antonangelo reports financial support was provided by Engineering and Physical Sciences Research Council. Fuoco and Rizzuto reports financial support was provided by Ministry for Universities and Research (MUR) of Italy. Alessio Fuoco is Editorial Board member of Separation and Purification Technology. Given his role as Editorial Board member, had no involvement in the peer review of this article and had no access to information regarding its peer review. Full responsibility for the editorial process for this article was delegated to another journal editor. If there are other authors, they declare that they have no known competing financial interests or personal relationships that could have appeared to influence the work reported in this paper.

Acknowledgements

C.R. and A.F are gratefully acknowledging the Ministry for Universities and Research (MUR) of Italy for financial support under the

program PRIN 2020 under the project “doMino” (2020P9KBKZ). The research leading to these results has received funding from the European Union’s Horizon Europe research and innovation programme under grant agreement No 101115488, project DAM4CO2 (J.C.J. and A.F.) and by UK Research and Innovation (UKRI) under the UK government’s Horizon Europe funding guarantee, grant number 10083164 (G.C.B. and M.C.). M.C., and A.R.A., gratefully acknowledge funding from the Engineering and Physical Sciences Research Council (EPSRC), Grant number: EP/T007362/1 “Novel polymers of intrinsic microporosity for heterogeneous base-catalysed reactions (HBC-PIMs)” and Swansea University. A.F. acknowledges funding from the CNR Program Short Term Mobility 2019.

Appendix A. Supplementary data

Supplementary data to this article can be found online at https://doi.org/10.1016/j.seppur.2025.135814.

Data availability

Data will be made available on request and are available at Zenodo at https://zenodo.org/communities/dam4co2/

References

[1] L. Fu, Z. Ren, W. Si, Q. Ma, W. Huang, K. Liao, Z. Huang, Y. Wang, J. Li, P. Xu, Research progress on CO2 capture and utilization technology, J CO_2 Util 66 (2022) 102260, https://doi.org/10.1016/j.jcou.2022.102260.
[2] S.G. Gizer, O. Polat, M.K. Ram, N. Sahiner, Recent developments in CO2 capture, utilization, related materials, and challenges, Int. J. Energy Res. 46 (12) (2022) 16241–16263, https://doi.org/10.1002/er.8347.
[3] H. Lin, L.S. White, K. Lokhandwala, R.W. Baker, Natural gas purification, Encyclopedia of Membrane Science and Technology (2013) 1–25, https://doi.org/10.1002/9781118522318.emst097.
[4] P. Pullumbi, F. Brandani, S. Brandani, Gas separation by adsorption: technological drivers and opportunities for improvement, Curr. Opin. Chem. Eng. 24 (2019) 131–142, https://doi.org/10.1016/j.coche.2019.04.008.
[5] Y.-T. Lin, J.-Y. Li, H.-H. Tseng, M.-Y. Wey, Insights into the role of polymer conformation on the cutoff size of carbon molecular sieving membranes for hydrogen separation and its novel pore size detection technology, ACS Appl. Mater. Interfaces (2021), https://doi.org/10.1021/acsami.0c21338.
[6] C.A. Grande, Advances in pressure swing adsorption for gas separation, International Scholarly Research Notices 2012 (2012), https://doi.org/10.5402/2012/982934.
[7] X. Chen, G. Liu, W. Jin, Natural gas purification by asymmetric membranes: An overview, Green Energy Environ. (2020), https://doi.org/10.1016/j.gee.2020.08.010.
[8] B. Zhu, S. He, Y. Yang, S. Li, C.H. Lau, S. Liu, L. Shao, Boosting membrane carbon capture via multifaceted polyphenol-mediated soldering, Nat. Commun. 14 (1) (2023) 1697, https://doi.org/10.1038/s41467-023-37479-9.
[9] Y. Dai, Z. Niu, W. Luo, Y. Wang, P. Mu, J. Li, A review on the recent advances in composite membranes for CO2 capture processes, Sep. Purif. Technol. 307 (2023) 122752, https://doi.org/10.1016/j.seppur.2022.122752.
[10] D. Wu, B. Zhang, J. Yuan, C. Yi, Structural engineering on 6FDA-Durene based polyimide membranes for highly selective gas separation, Sep. Purif. Technol. 316 (2023) 123786, https://doi.org/10.1016/j.seppur.2023.123786.
[11] A. Imtiaz, M.H. Othman, A. Jilani, I.U. Khan, R. Kamaludin, J. Iqbal, A.G. Al-Sehemi, Challenges, opportunities and future directions of membrane Technology for Natural gas Purification: a critical review, Membranes 12 (7) (2022), https://doi.org/10.3390/membranes12070646.
[12] A.G. Olabi, A.H. Alami, M. Ayoub, H. Aljaghoub, S. Alasad, A. Inayat, M. A. Abdelkareem, K.-J. Chae, E.T. Sayed, Membrane-based carbon capture: recent progress, challenges, and their role in achieving the sustainable development goals, Chemosphere 320 (2023) 137996, https://doi.org/10.1016/j.chemosphere.2023.137996.
[13] D. Singh Gill, S. Mariam Abraham, Feasibility of CO2 Sequestration in Concrete Containing Recycled Aggregates, Materials Today, Proceedings, 2023, https://doi.org/10.1016/j.matpr.2023.03.186.
[14] R. Khalilpour, K. Mumford, H. Zhai, A. Abbas, G. Stevens, E.S. Rubin, Membrane-based carbon capture from flue gas: a review, J. Clean. Prod. 103 (2015) 286–300, https://doi.org/10.1016/j.jclepro.2014.10.050.
[15] I.A. Qazi, A.A. Abd, M.M. Hasan, M.R. Othman, Optimizing hydrogen purification performance by membrane from industrial waste of methanol production, Chem. Eng. J. Adv. 14 (2023) 100490, https://doi.org/10.1016/j.ceja.2023.100490.
[16] C.E. Powell, G.G. Qiao, Polymeric CO2/N2 gas separation membranes for the capture of carbon dioxide from power plant flue gases, J. Membr. Sci. 279 (1) (2006) 1–49, https://doi.org/10.1016/j.memsci.2005.12.062.
[17] L.M. Robeson, Correlation of separation factor versus permeability for polymeric membranes, J. Membr. Sci. 62 (2) (1991) 165–185, https://doi.org/10.1016/0376-7388(91)80060-J.
[18] L.M. Robeson, The upper bound revisited, J. Membr. Sci. 320 (1–2) (2008) 390–400, https://doi.org/10.1016/j.memsci.2008.04.030.
[19] R. Swaidan, B. Ghanem, I. Pinnau, Fine-tuned intrinsically Ultramicroporous polymers redefine the permeability/selectivity upper bounds of membrane-based air and hydrogen separations, ACS Macro Lett. 4 (9) (2015) 947–951, https://doi.org/10.1021/acsmacrolett.5b00512.
[20] B. Comesaña-Gándara, J. Chen, C.G. Bezzu, M. Carta, I. Rose, M.-C. Ferrari, E. Esposito, A. Fuoco, J.C. Jansen, N.B. McKeown, Redefining the Robeson upper bounds for CO 2/CH 4 and CO 2/N 2 separations using a series of ultrapermeable benzotriptycene-based polymers of intrinsic microporosity, Energy Environ. Sci. 12 (9) (2019) 2733–2740, https://doi.org/10.1039/C9EE01384A.
[21] A. Ismail, R. Rahim, W. Rahman, Characterization of polyethersulfone/Matrimid® 5218 miscible blend mixed matrix membranes for O2/N2 gas separation, Sep. Purif. Technol. 63 (1) (2008) 200–206, https://doi.org/10.1016/j.seppur.2008.05.007.
[22] J.D. Wind, D.R. Paul, W.J. Koros, Natural gas permeation in polyimide membranes, J. Membr. Sci. 228 (2) (2004) 227–236, https://doi.org/10.1016/j.memsci.2003.10.011.
[23] R.S. Murali, K.Y. Rani, T. Sankarshana, A. Ismail, S. Sridhar, Separation of binary mixtures of propylene and propane by facilitated transport through silver incorporated poly (ether-block-amide) membranes, Oil & Gas Science and Technology–Revue d’IFP Energies nouvelles 70 (2) (2015) 381–390, https://doi.org/10.2516/ogst/2013190.
[24] A. Jomekian, R.M. Behbahani, T. Mohammadi, A. Kargari, CO2/CH4 separation by high performance CO-casted ZIF-8/Pebax 1657/PES mixed matrix membrane, J. Nat. Gas Eng. 31 (2016) 562–574, https://doi.org/10.1016/j.jngse.2016.03.067.
[25] M. Longo, M. Monteleone, E. Esposito, A. Fuoco, E. Tocci, M.-C. Ferrari, B. Comesaña-Gándara, R. Malpass-Evans, N.B. McKeown, J.C. Jansen, Thin film composite membranes based on the polymer of intrinsic microporosity PIM-EA (Me2)-TB blended with Matrimid® 5218, Membranes 12 (9) (2022) 881, https://doi.org/10.3390/membranes12090881.
[26] N.E. León, Z. Liu, M. Irani, W.J. Koros, How to get the best gas separation membranes from state-of-the-art glassy polymers, Macromolecules 55 (5) (2022) 1457–1473, https://doi.org/10.1021/acs.macromol.1c01758.
[27] F.N. Al-Rowaili, M. Khaled, A. Jamal, U. Zahid, Mixed matrix membranes for H2/CO2 gas separation- a critical review, Fuel 333 (2023) 126285, https://doi.org/10.1016/j.fuel.2022.126285.
[28] X. Tan, S. Robijns, R. Thür, Q. Ke, N. De Witte, A. Lamaire, Y. Li, I. Aslam, D. Van Havere, T. Donckels, T. Van Assche, V. Van Speybroeck, M. Dusselier, I. Vankelecom, Truly combining the advantages of polymeric and zeolite membranes for gas separations, Science 378 (6625) (2022) 1189–1194, https://doi.org/10.1126/science.ade1411.
[29] S. Li, Y.-J. Sun, Z.-X. Wang, C.-G. Jin, M.-J. Yin, Q.-F. An, Rapid Fabrication of High-Permeability Mixed Matrix Membranes at Mild Condition for CO2 Capture, Small (2023) 2208177, https://doi.org/10.1002/smll.202208177.
[30] S. La Cognata, R. Mobili, C. Milanese, M. Boiocchi, M. Gaboardi, D. Armentano, J. C. Jansen, M. Monteleone, A.R. Antonangelo, M. Carta, CO2 separation by imide/imine organic cages, Chem. Eur. J. 28 (49) (2022) e202201631, https://doi.org/10.1002/chem.202201631.
[31] A. Imtiaz, M.H.D. Othman, A. Jilani, I.U. Khan, R. Kamaludin, O. Samuel, ZIF-filler incorporated mixed matrix membranes (MMMs) for efficient gas separation: a review, J. Environ. Chem. Eng. (2022) 108541, https://doi.org/10.1016/j.jece.2022.108541.
[32] Y. Cheng, Y. Ying, S. Japip, S.-D. Jiang, T.-S. Chung, S. Zhang, D. Zhao, Advanced porous materials in mixed matrix membranes, Adv. Mater. 30 (47) (2018) 1802401, https://doi.org/10.1002/adma.201802401.
[33] A.R. Antonangelo, N. Hawkins, E. Tocci, C. Muzzi, A. Fuoco, M. Carta, Tröger’s base network polymers of intrinsic microporosity (TB-PIMs) with tunable pore size for heterogeneous catalysis, J. Am. Chem. Soc. 144 (34) (2022) 15581–15594, https://doi.org/10.1021/jacs.2c04739.
[34] F. Marken, M. Carta, N.B. McKeown, Polymers of intrinsic microporosity in the Design of Electrochemical Multicomponent and Multiphase Interfaces, Anal. Chem. 93 (3) (2021) 1213–1220, https://doi.org/10.1021/acs.analchem.0c04554.
[35] E. Al-Hetlani, M.O. Amin, C.G. Bezzu, M. Carta, Spirobifluorene-based polymers of intrinsic microporosity for the adsorption of methylene blue from wastewater: effect of surfactants, R. Soc. Open Sci. 7 (9) (2020) 200741, https://doi.org/10.1098/rsos.200741.
[36] N.B. McKeown, P.M. Budd, Polymers of intrinsic microporosity (PIMs): organic materials for membrane separations, heterogeneous catalysis and hydrogen storage, Chem. Soc. Rev. 35 (8) (2006) 675–683, https://doi.org/10.1039/B600349D.
[37] M. Carta, R. Malpass-Evans, M. Croad, Y. Rogan, J.C. Jansen, P. Bernardo, F. Bazzarelli, N.B. McKeown, An efficient polymer molecular sieve for membrane gas separations, Science 339 (6117) (2013) 303–307, https://doi.org/10.1126/science.1228032.
[38] C.H. Lau, K. Konstas, C.M. Doherty, S.J. Smith, R. Hou, H. Wang, M. Carta, H. Yoon, J. Park, B.D. Freeman, Tailoring molecular interactions between microporous polymers in high performance mixed matrix membranes for gas separations, Nanoscale 12 (33) (2020) 17405–17410, https://doi.org/10.1039/D0NR04801A.
[39] C. Atalay-Oral, M. Tatlier, Effects of structural properties of fillers on performances of Matrimid® 5218 mixed matrix membranes, Sep. Purif. Technol. 236 (2020) 116277, https://doi.org/10.1016/j.seppur.2019.116277.

[40] H. Zhou, C. Rayer, A.R. Antonangelo, N. Hawkins, M. Carta, Adjustable functionalization of hyper-cross-linked polymers of intrinsic microporosity for enhanced CO2 adsorption and selectivity over N2 and CH4, ACS Appl. Mater. Interfaces 14 (18) (2022) 20997–21006, https://doi.org/10.1021/acsami.2c02604.
[41] T. Ikai, T. Yoshida, K.-I. Shinohara, T. Taniguchi, Y. Wada, T.M. Swager, Triptycene-based ladder polymers with one-handed helical geometry, J. Am. Chem. Soc. 141 (11) (2019) 4696–4703, https://doi.org/10.1021/jacs.8b13865.
[42] M.-J. Gu, Y.-F. Wang, Y. Han, C.-F. Chen, Recent advances on triptycene derivatives in supramolecular and materials chemistry, Org. Biomol. Chem. 19 (46) (2021) 10047–10067, https://doi.org/10.1039/D1OB01818C.
[43] C.H. Lau, T.-D. Lu, S.-P. Sun, X. Chen, M. Carta, D.M. Dawson, Continuous flow knitting of a triptycene hypercrosslinked polymer, Chem. Commun. 55 (59) (2019) 8571–8574, https://doi.org/10.1039/C9CC03731D.
[44] E. Al-Hetlani, M.O. Amin, A.R. Antonangelo, H. Zhou, M. Carta, Triptycene and triphenylbenzene-based polymers of intrinsic microporosity (PIMs) for the removal of pharmaceutical residues from wastewater, Microporous Mesoporous Mater. 330 (2022) 111602, https://doi.org/10.1016/j.micromeso.2021.111602.
[45] Y. Liu, S. Wu, G. Wang, G. Yu, J. Guan, C. Pan, Z. Wang, Control of porosity of novel carbazole-modified polytriazine frameworks for highly selective separation of CO2–N2, J Mater Chem A 2 (21) (2014) 7795–7801, https://doi.org/10.1039/C4TA00298A.
[46] R.-B. Lin, Y. He, P. Li, H. Wang, W. Zhou, B. Chen, Multifunctional porous hydrogen-bonded organic framework materials, Chem. Soc. Rev. 48 (5) (2019) 1362–1389, https://doi.org/10.1039/C8CS00155C.
[47] M. Mon, R. Bruno, E. Tiburcio, A. Grau-Atienza, A. Sepúlveda-Escribano, E. V. Ramos-Fernandez, A. Fuoco, E. Esposito, M. Monteleone, J.C. Jansen, J. Cano, J. Ferrando-Soria, D. Armentano, E. Pardo, Efficient Gas Separation and Transport Mechanism in Rare Hemilabile Metal–Organic Framework, Chem. Mater. 31 (15) (2019) 5856–5866, https://doi.org/10.1021/acs.chemmater.9b01995.
[48] D.R. Paul, Effect of immobilizing adsorption on the diffusion time lag, journal of polymer science part A-2: polymer, Physics 7 (10) (1969) 1811–1818, https://doi.org/10.1002/pol.1969.160071015.
[49] Z. Grzywna, J. Podkowka, Effect of immobilizing adsorption on mass transport through polymer films, J. Membr. Sci. 8 (1) (1981) 23–31, https://doi.org/10.1016/S0376-7388(00)82136-5.
[50] C. Rizzuto, F. Nardelli, M. Monteleone, L. Calucci, C.G. Bezzu, M. Carta, E. Tocci, E. Esposito, G. De Luca, B. Comesaña-Gándara, N.B. McKeown, B. Sayginer, P. M. Budd, J.C. Jansen, A. Fuoco, Unravelling the origin of enhanced CO2 selectivity in amine-PIM-1 during mixed gas permeation, J Mater Chem A 13 (23) (2025) 17865–17876, https://doi.org/10.1039/D4TA08839E.
[51] T.D. Duong, S.A. Sapchenko, I. da Silva, H.G.W. Godfrey, Y. Cheng, L.L. Daemen, P. Manuel, M.D. Frogley, G. Cinque, A.J. Ramirez-Cuesta, S. Yang, M. Schröder, Observation of binding of carbon dioxide to nitro-decorated metal–organic frameworks, Chem. Sci. 11 (20) (2020) 5339–5346, https://doi.org/10.1039/C9SC04294F.
[52] K. Mizrahi Rodriguez, F.M. Benedetti, N. Roy, A.X. Wu, Z.P. Smith, Sorption-enhanced mixed-gas transport in amine functionalized polymers of intrinsic microporosity (PIMs), J Mater Chem A 9 (41) (2021) 23631–23642, https://doi.org/10.1039/D1TA06530K.
[53] V. Teplyakov, P. Meares, Correlation aspects of the selective gas permeabilities of polymeric materials and membranes, Gas Sep. Purif. 4 (2) (1990) 66–74, https://doi.org/10.1016/0950-4214(90)80030-O.
[54] L. Liu, E.S. Sanders, S.S. Kulkarni, D.J. Hasse, W.J. Koros, Sub-ambient temperature flue gas carbon dioxide capture via Matrimid® hollow fiber membranes, J. Membr. Sci. 465 (2014) 49–55, https://doi.org/10.1016/j.memsci.2014.03.060.
[55] S.A. Gülmüs, L. Yilmaz, Effect of temperature and membrane preparation parameters on gas permeation properties of polymethacrylates, J. Polym. Sci. B Polym. Phys. 45 (22) (2007) 3025–3033, https://doi.org/10.1002/polb.21258.
[56] C.M. Zimmerman, W.J. Koros, Polypyrrolones for membrane gas separations. II. Activation energies and heats of sorption, J. Polym. Sci. B Polym. Phys. 37 (12) (1999) 1251–1265.
[57] A. Fuoco, B. Comesaña-Gándara, M. Longo, E. Esposito, M. Monteleone, I. Rose, C. G. Bezzu, M. Carta, N.B. McKeown, J.C. Jansen, Temperature dependence of gas permeation and diffusion in Triptycene-based Ultrapermeable polymers of intrinsic microporosity, ACS Appl. Mater. Interfaces 10 (42) (2018) 36475–36482, https://doi.org/10.1021/acsami.8b13634.
[58] W.J. Koros, C. Zhang, Materials for next-generation molecularly selective synthetic membranes, Nat. Mater. 16 (3) (2017) 289–297, https://doi.org/10.1038/nmat4805.